Mediterr. J. Math. 13 (2016), 2319–2336
DOI 10.1007/s00009-015-0594-3
1660-5446/16/042319-18
published online June 17, 2015

Mediterranean Journal of Mathematics

Shifted Legendre Collocation Method for the Flow and Heat Transfer due to a Stretching Sheet Embedded in a Porous Medium with Variable Thickness, Variable Thermal Conductivity and Thermal Radiation

M. M. Khader

Abstract. This paper is devoted to introduce a numerical simulation with a theoretical study for flow of a Newtonian fluid over an impermeable stretching sheet which embedded in a porous medium with a power law surface velocity and variable thickness in the presence of thermal radiation. The flow is caused by a non-linear stretching of a sheet. Thermal conductivity of the fluid is assumed to vary linearly with temperature. The governing PDEs are transformed into a system of coupled non-linear ODEs which are using appropriate boundary conditions for various physical parameters. The proposed method is based on replacement of the unknown function by truncated series of well known shifted Legendre expansion of functions. An approximate formula of the integer derivative is introduced. Special attention is given to study the convergence analysis and derive an upper bound of the error of the presented approximate formula. The introduced method converts the proposed equation by means of collocation points to a system of algebraic equations with shifted Legendre coefficients. Thus, by solving this system of equations, the shifted Legendre coefficients are obtained. The effects of the porous parameter, the wall thickness parameter, the radiation parameter, thermal conductivity parameter and the Prandtl number on the flow and temperature profiles are presented. Moreover, the local skin-friction and Nusselt numbers are presented. Comparison of obtained numerical results is made with previously published results in some special cases, and excellent agreement is noted. The results attained in this paper confirm the idea that proposed method is powerful mathematical tool and it can be applied to a large class of linear and nonlinear problems arising in different fields of science and engineering.

Mathematics Subject Classification. 41A04, 65N20, 76S02.

Keywords. Newtonian fluid, stretching sheet, thermal radiation, variable thermal conductivity, variable thickness, Legendre collocation method, convergence analysis.

1. Introduction

The study of flow and heat transfer of a Newtonian fluid over a stretching surface issuing from slit has gained considerable attention of many researchers due to its importance in many industrial applications, such as, extraction of polymer sheet, wire drawing, paper production, glass-fiber production, hot rolling, solidification of liquid crystals, petroleum production, continuous cooling and fibers spinning, exotic lubricants and suspension solutions. Much work on the boundary-layer Newtonian fluids has been carried out both experimentally and theoretically. Crane [1] was the first one who studied the stretching problem taking into account the fluid flow over a linearly stretched surface. There has been a great deal of the work done on Newtonian fluid flow and heat transfer over a stretching surface, but only a few recent studies are cited here. Gupta and Gupta [2] analyzed the stretching problem with a constant surface temperature, while Soundalgekar and Ramana [3] have investigated the constant surface velocity case with a power-law temperature variation. Grubka and Bobba [4] have analyzed the stretching problem for a surface moving with a linear velocity and with a variable surface temperature. Chen and Char [5] investigated the heat transfer characteristics over a continuous stretching sheet with variable surface temperature. Using the homotopy analysis method (HAM), series solutions were obtained by Hayat et al. [6] for the stretching sheet problem with mixed convection.

Despite the practical importance of the flow in a porous medium, all the above-mentioned works do not however consider the situations where the flow in fluid-saturated porous media arise. The study of the flow in fluid-saturated porous media due to a stretching sheet is important in engineering problems, such as the design of building components for energy consideration, soil science, mechanical engineering, control of pollutant spread in groundwater, thermal insulation systems, compact heat exchangers, solar power collectors and food industries. Because of such important practical applications, many investigators have modeled the behavior of a boundary layer flow embedded in a porous medium. Cheng and Minkowycz [7] studied the problem of free convection about a vertical impermeable flat plate in a Darcy porous medium. Elbashbeshy and Bazid [8] studied flow and heat transfer in a porous medium over a stretching surface with internal heat generation and suction/blowing when the surface is held at a constant temperature. Cortell [9] has presented an analytical solution of the problem considered by Elbashbeshy and Bazid [8] considering the constant surface temperature and prescribed surface temperature. Recently, Hayat et al. [10] used HAM to give analytic solution for flow through porous medium.

Radiative heat transfer flow is very important in manufacturing industries for the design of reliable equipments, nuclear plants, gas turbines and various propulsion devices for aircraft, missiles, satellites and space vehicles. Also, the effect of thermal radiation on the forced and free convection flows are important in the context of space technology and processes involving high temperature. Based on these applications, Hossain et al. [11] and Elbashbeshy and Demain [12] have studied the thermal radiation of a gray

fluid which is emitting and absorbing radiation in non-scattering medium. Abel and Mahesha [13] studied the effect of radiation in different situations. Recently, Battaler [14] has studied the effect of thermal radiation on the laminar boundary layer about a flat plate.

Historically, the study on boundary layer flows over a stretching sheet with variable thickness was studied by Fang et al. [15]. However, so far no attention has been given to the effects of the non-flatness on the stretching sheet problems considering a variable sheet thickness. The purpose of the present paper is to investigate the numerical solution for the variable thermal conductivity effect on the flow and heat transfer of a Newtonian fluid-saturated porous medium over a stretching sheet with variable thickness in the presence of thermal radiation. For more details see ([16,17]).

Legendre polynomials are well known family of orthogonal polynomials on the interval $[-1, 1]$ that have many applications. They are widely used because of their good properties in the approximation of functions [18–24]. Orthogonal polynomials have a great variety and wealth of properties. Some of these properties take a very concise form in the case of the Legendre polynomials, making Legendre polynomials of leading importance among orthogonal polynomials. The Legendre polynomials belong to an exclusive band of orthogonal polynomials, known as Jacobi polynomials, which correspond to weight functions of the form $(1 - x)^{\alpha}(1 + x)^{\beta}$ and which are solutions of Sturm–Liouville equations [21].

The Legendre collocation method is used to solve many problems, in more papers such as [18–24]. In this work, we use the properties of the Legendre polynomials to derive an approximate formula of the integer derivative $D^{(n)}y(x)$ and estimate an error upper bound of this formula, then we use this formula to solve numerically the proposed problem.

2. Formulation of the Problem

Consider a steady, two-dimensional boundary layer flow of an incompressible Newtonian fluid over a continuously impermeable stretching sheet embedded in a porous medium. The origin is located at a slit, through which the sheet (see Fig. 1) is drawn through the fluid medium. The x-axis is chosen along the sheet and y-axis is taken normal to it. The stretching surface has the velocity $U_w = U_0(x + b)^m$, where U_0 is the reference velocity. We assume that the sheet is not flat in which it is specified as $y = A(x + b)^{\frac{1-m}{2}}$, where A is a very small constant so that the sheet is sufficiently thin and m is the velocity power index. We must observe that our problem is valid only for $m \neq 1$, because for $m = 1$, the problem reduces to a flat sheet. Likewise, the fluid properties are assumed to be constant except for thermal conductivity variations in the temperature.

Making the usual boundary layer approximations for the Newtonian fluid, the steady two-dimensional boundary-layer equations taking into account the thermal radiation effect in the energy equation can be written as

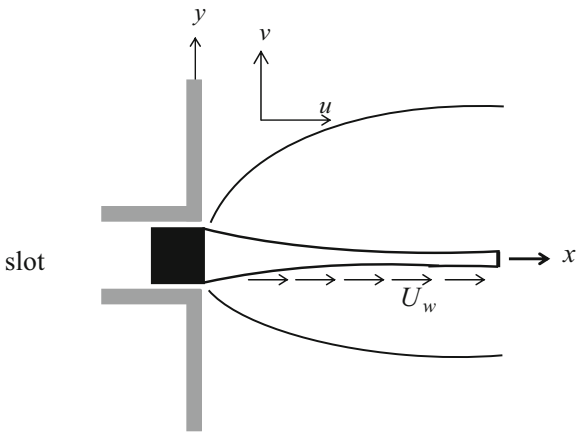

Figure 1. Schematic of a stretching sheet with variable sheet thickness

$$\frac{\partial u}{\partial x} + \frac{\partial v}{\partial y} = 0, \tag{1}$$

$$u\frac{\partial u}{\partial x} + v\frac{\partial u}{\partial y} = \nu\frac{\partial^2 u}{\partial y^2} - \frac{\mu}{\rho k}u, \tag{2}$$

$$\rho c_p\left(u\frac{\partial T}{\partial x} + v\frac{\partial T}{\partial y}\right) = \frac{\partial}{\partial y}\left(\kappa\frac{\partial T}{\partial y}\right) - \frac{\partial q_r}{\partial y}, \tag{3}$$

where u and v are the velocity components in x and y directions, respectively. ρ and κ are the fluid density and the thermal conductivity, respectively. T is the temperature of the fluid, ν is the fluid kinematic viscosity, c_p is the specific heat at constant pressure, μ is the fluid viscosity, k is the permeability of the porous medium and q_r is the radiative heat flux.

The radiative heat flux q_r is employed according to Rosseland approximation [25] such that

$$q_r = -\frac{4\sigma^*}{3k^*}\frac{\partial T^4}{\partial y}, \tag{4}$$

where $\sigma^* = 5.6697 \times 10^{-8}\ Wm^{-2}K^{-4}$ is the Stefan–Boltzmann constant and k^* is the mean absorption coefficient. Following Raptis [26], we assume that the temperature differences within the flow are sufficiently small such that T^4 may be expressed as a linear function of the temperature. Expanding T^4 in a Taylor series about T_∞ and neglecting higher-order terms, we have

$$T^4 \cong 4T_\infty^3 T - 3T_\infty^4. \tag{5}$$

The physical and mathematical advantage of the Rosseland formula (5) consists of the fact that it can be combined with Fourier's second law of conduction to an effective conduction-radiation flux q_{eff} in the form

$$q_{\text{eff}} = -\left(\kappa + \frac{16\sigma^* T_\infty^3}{3k^*}\right)\frac{\partial T}{\partial y} = -\kappa_{\text{eff}}\frac{\partial T}{\partial y}, \tag{6}$$

where $\kappa_{\text{eff}} = \kappa + \frac{16\sigma^* T_\infty^3}{3k^*}$ is the effective thermal conductivity. So, the steady energy balance equation including the net contribution of the radiation emitted from the hot wall and absorbed in the colder fluid, takes the form

$$\rho c_p \left(u\frac{\partial T}{\partial x} + v\frac{\partial T}{\partial y} \right) = \frac{\partial}{\partial y}(\kappa_{\text{eff}} \frac{\partial T}{\partial y}). \tag{7}$$

To obtain similarity solutions, it is assumed that the permeability of the porous medium $k(x)$ is of the form

$$k(x) = k_0(x+b)^{1-m}, \tag{8}$$

where k_0 is the permeability parameter. The boundary conditions can be written as

$$u\left(x, A(x+b)^{\frac{1-m}{2}}\right) = U_0(x+b)^m, \quad v\left(x, A(x+b)^{\frac{1-m}{2}}\right) = 0,$$
$$T\left(x, A(x+b)^{\frac{1-m}{2}}\right) = T_w, \tag{9}$$

$$u(x,\infty) = 0, \qquad T(x,\infty) = T_\infty. \tag{10}$$

The mathematical analysis of the problem is simplified by introducing the following dimensionless coordinates

$$\zeta = y\sqrt{U_0(\frac{m+1}{2})\left(\frac{(x+b)^{m-1}}{\nu}\right)}, \quad \psi(x,y) = \sqrt{\nu U_0(\frac{2}{m+1})(x+b)^{m+1}}F(\zeta),$$
$$\Theta(\zeta) = \left(\frac{T-T_\infty}{T_w - T_\infty}\right), \tag{11}$$

where ζ is the similarity variable, $\psi(x,y)$ is the stream function which is defined in the classical form as $u = \partial\psi/\partial y$ and $v = -\partial\psi/\partial x$ and $\Theta(\zeta)$ is the dimensionless temperature.

In this study, the equation for the dimensionless thermal conductivity κ is generalized for the temperature dependence as follows ([27–29])

$$\kappa = \kappa_\infty(1 + \epsilon\Theta), \tag{12}$$

where κ_∞ is the ambient thermal conductivity and ϵ is the thermal conductivity parameter.

Upon using these variables, the boundary layer governing equations (1)–(3) can be written in a non-dimensional following form

$$F''' + FF'' - \frac{2m}{m+1}F'^2 - DF' = 0, \tag{13}$$

$$\left(\frac{1+R}{Pr}\right)\left((1+\epsilon\Theta)\Theta'' + \epsilon\Theta'^2\right) + F\Theta' = 0, \tag{14}$$

where $D = \frac{2\nu}{k_0 U_0(m+1)}$ is the porous parameter, $Pr = \frac{\mu c_p}{\kappa_\infty}$ is the Prandtl number and $R = \frac{16\sigma^* T_\infty^3}{3k^*\kappa_\infty}$ is the radiation parameter. The transformed boundary conditions are

$$F(\alpha) = \alpha\left(\frac{1-m}{1+m}\right), \quad F'(\alpha) = 1, \quad \Theta(\alpha) = 1, \tag{15}$$

$$F'(\infty) = 0, \quad \Theta(\infty) = 0, \tag{16}$$

where $\alpha = A\sqrt{\frac{U_0(m+1)}{2\nu}}$ is a parameter related to the thickness of the wall and $\zeta = \alpha = A\sqrt{\frac{U_0(m+1)}{2\nu}}$ indicates the plate surface. In order to facilitate the computation, we define $F(\zeta) = F(\eta-\alpha) = f(\eta)$ and $\Theta(\zeta) = \Theta(\eta-\alpha) = \theta(\eta)$. The similarity equation and the associated boundary conditions become

$$f''' + ff'' - \frac{2m}{m+1}f'^2 - Df' = 0, \tag{17}$$

$$\left(\frac{1+R}{Pr}\right)\left((1+\epsilon\theta)\theta'' + \epsilon\theta'^2\right) + f\theta' = 0, \tag{18}$$

$$f(0) = \alpha\left(\frac{1-m}{1+m}\right), \qquad f'(0) = 1, \qquad \theta(0) = 1, \tag{19}$$

$$f'(\infty) = 0, \qquad \theta(\infty) = 0, \tag{20}$$

where the prime denotes differentiation with respect to η. Based on the variable transformation, the solution domain will be fixed from 0 to ∞.

The physical quantities of primary interest are the local skin-friction coefficient Cf and the local Nusselt number Nu which are defined as

$$Cf = -2\sqrt{\frac{m+1}{2}}Re_x^{\frac{-1}{2}}f''(0), \qquad Nu = -\sqrt{\frac{m+1}{2}}Re_x^{\frac{1}{2}}\theta'(0), \tag{21}$$

where $Re_x = \frac{U_w X}{\nu}$ is the local Reynolds number and $X = x + b$.

3. An Approximate Formula of the Integer Derivative for Legendre Polynomials Expansion

The well known Legendre polynomials are defined on the interval $[-1, 1]$ and can be determined with the aid of the following recurrence formula [21]

$$L_{k+1}(z) = \frac{2k+1}{k+1}\,z\,L_k(z) - \frac{k}{k+1}L_{k-1}(z), \qquad k = 1, 2, \ldots,$$

where $L_0(z) = 1$ and $L_1(z) = z$. In order to use these polynomials on the interval $[0, \hbar]$ we define the so called shifted Legendre polynomials by introducing the change of variable $z = (2/\hbar)t - 1$. Let the shifted Legendre polynomials $L_k((2/\hbar)t - 1)$ be denoted by $L_k^*(t)$. Then $L_k^*(t)$ can be obtained as follows:

$$L_{k+1}^*(t) = \frac{(2k+1)((2/\hbar)t-1)}{(k+1)}\,L_k^*(t) - \frac{k}{k+1}\,L_{k-1}^*(t), \qquad k = 1, 2, \ldots,$$

where $L_0^*(t) = 1$ and $L_1^*(t) = (2/\hbar)t - 1$. The analytic form of the shifted Legendre polynomials $L_k^*(t)$ of degree k is given by

$$L_k^*(t) = \sum_{i=0}^{k}(-1)^{k+i}\frac{(k+i)!}{\hbar^i(k-i)!(i!)^2}\,t^i. \tag{22}$$

Note that $L_k^*(0) = (-1)^k$ and $L_k^*(\hbar) = 1$. The orthogonality condition is:

$$\int_0^{\hbar} L_i^*(t)L_j^*(t)\,\mathrm{d}t = \begin{cases} \frac{\hbar}{2i+1}, & i = j; \\ 0, & i \neq j. \end{cases}$$

The function $y(t)$, which is square integrable in $[0, 1]$, may be expressed in terms of shifted Legendre polynomials as

$$y(t) = \sum_{i=0}^{\infty} c_i L_i^*(t), \tag{23}$$

where the coefficients c_i are given by

$$c_i = \frac{2i+1}{\hbar} \int_0^{\hbar} y(t) L_i^*(t)\, \mathrm{d}t, \qquad i = 0, 1, \ldots . \tag{24}$$

In practice, only the first $(M+1)$-terms of shifted Legendre polynomials are considered. Then we have

$$y_M(t) = \sum_{i=0}^{M} c_i L_i^*(t). \tag{25}$$

The main approximate formula of the integer derivative is given in the following theorem.

In this section, special attention is given to study the convergence analysis and evaluate an upper bound for the proposed approximate formula.

Theorem 1. *The integer derivative of order n for the shifted Legendre polynomials can be expressed in terms of the shifted Legendre polynomials themselves in the following form*

$$D^{(n)}(L_i^*(t)) = \sum_{k=n}^{i} \sum_{j=0}^{k-n} \Theta_{i,j,k}\, L_j^*(t), \tag{26}$$

where

$$\Theta_{i,j,k} = \frac{(-1)^{i+k}(i+k)!(2j+1)}{\hbar^i (i-k)!(k)!(k-n)!} \times \sum_{r=0}^{j} \frac{(-1)^{j+r}(j+r)!}{(j-r)!\,(r!)^2 (k-n+r+1)}, \quad j = 0, 1, \ldots \tag{27}$$

Proof. Since the differentiation is a linear operation, then from (25) we get

$$y_M^{(n)}(t) = \sum_{i=0}^{M} c_i D^{(n)}(L_i^*(t)). \tag{28}$$

From the formula (22) we can obtain $D^{(n)} L_i^*(t) = 0, \quad i = 0, 1, \ldots, n-1$.

Therefore, for $i = n, n+1, \ldots, M$ and formula (22) we get

$$D^{(n)} L_i^*(t) = \sum_{k=0}^{i} \frac{(-1)^{i+k}(i+k)!}{\hbar^i (i-k)!(k!)^2} D^{(n)}(t^k) = \sum_{k=n}^{i} \frac{(-1)^{i+k}(i+k)!}{\hbar^i (i-k)! k! (k-n)!} t^{k-n}. \tag{29}$$

A combination of Eqs. (28) and (29) leads to the following result

$$y_M^{(n)}(t) = \sum_{i=n}^{M} \sum_{k=n}^{i} c_i\, \gamma_{i,k}^{(n)} t^{k-n}, \tag{30}$$

where $\gamma_{i,k}^{(n)}$ is given by $\gamma_{i,k}^{(n)} = \frac{(-1)^{(i+k)}(i+k)!}{\hbar^i (i-k)!k!(k-n)!}$.

Using the properties of the shifted Legendre polynomials [21], then t^{k-n} in (29) can be expanded in the following form

$$t^{k-n} = \sum_{j=0}^{k-n} c_{kj} L_j^*(t), \tag{31}$$

where c_{kj} can be obtained using (24) such that $y(t) = t^{k-n}$, then we can claim the following

$$c_{kj} = \frac{2j+1}{\hbar} \int_0^{\hbar} t^{k-n} L_j^*(t) \mathrm{d}t, \qquad j = 0, 1, \ldots.$$

$$\text{But at } j = 0 \text{ we have,} \quad c_{k0} = \frac{1}{\hbar} \int_0^{\hbar} t^{k-n} \mathrm{d}t = \frac{\hbar^{(k-n)}}{k-n+1},$$

also, for any j, and using the formula (22), we can claim

$$c_{kj} = (2j+1) \sum_{r=0}^{j} (-1)^{j+r} \frac{(j+r)!}{\hbar^j (j-r)!(r!)^2 (k-n+r+1)}, \qquad j = 1, 2, \ldots,$$

employing Eqs. (29) and (31) gives

$$D^{(n)}(L_i^*(t)) = \sum_{k=n}^{i} \sum_{j=0}^{k-n} \Theta_{i,j,k} L_j^*(t), \quad i = n, n+1, \ldots,$$

where $\Theta_{i,j,k}$ is given in (27) and this completes the proof of the theorem. □

Now, the combination of Eqs. (23), (25) and (26) and $|L_j^*(t)| \leq 1$, with subtracting the truncated series from the infinite series, bounding each term in the difference, and summing we can prove the following lemma.

Lemma 1. *The error* $|E_T(M)| = |y^{(n)}(t) - y_M^{(n)}(t)|$ *in approximating* $y^{(n)}(t)$ *by* $y_M^{(n)}(t)$ *is bounded by*

$$|E_T(M)| \leq \Big| \sum_{i=M+1}^{\infty} c_i \Big(\sum_{k=n}^{i} \sum_{j=0}^{k-n} \Theta_{i,j,k} \Big) \Big|.$$

4. Procedure Solution

In this section, we present the proposed method to solve numerically the system of ordinary differential equations of the form (17)–(18). The unknown functions $f(\eta)$ and $\theta(\eta)$ may be expanded by finite series of shifted Legendre polynomials as the following approximation

$$f_M(\eta) = \sum_{i=0}^{M} c_i L_i^*(\eta), \quad \theta_M(\eta) = \sum_{i=0}^{M} d_i L_i^*(\eta). \tag{32}$$

Table 1. Comparison of the numerical value of $-f''(0)$, obtained by Legendre collocation method for $\alpha = 0.5, \lambda = 0$ with Fang et al. [15]

m	10.00	9.00	7.00	5.00	3.00	2.00	1.00	0.50	0.00	-0.50
$-f''(0)$	1.0603	1.0589	1.0550	1.0486	1.0359	1.0234	1.0000	0.9799	0.9576	1.1667
Present work	1.0603	1.0588	1.0551	1.0486	1.0358	1.0234	1.0000	0.9798	0.9577	1.1666

From Eqs. (17), (18), (32) and the formula (30) we have

$$\sum_{i=3}^{M}\sum_{k=3}^{i} c_i\,\gamma_{i,k}^{(3)}\,\eta^{k-3} + \sum_{i=0}^{M} c_i L_i^*(\eta)\left(\sum_{i=2}^{M}\sum_{k=2}^{i} c_i\,\gamma_{i,k}^{(2)}\,\eta^{k-2}\right) - \left(\frac{2m}{1+m}\right)\left(\sum_{i=1}^{M}\sum_{k=1}^{i} c_i\,\gamma_{i,k}^{(1)}\,\eta^{k-1}\right)^2 - D\sum_{i=1}^{M}\sum_{k=1}^{i} c_i\,\gamma_{i,k}^{(1)}\,\eta^{k-1} = 0, \quad (33)$$

$$\sum_{i=2}^{M}\sum_{k=2}^{i} d_i\,\gamma_{i,k}^{(2)}\,\eta^{k-2} + \epsilon\sum_{i=0}^{M} d_i L_i^*(\eta)\left(\sum_{i=2}^{M}\sum_{k=2}^{i} d_i\,\gamma_{i,k}^{(2)}\,\eta^{k-2}\right) + \epsilon\left(\sum_{i=1}^{M}\sum_{k=1}^{i} d_i\,\gamma_{i,k}^{(1)}\,\eta^{k-1}\right)^2 + \frac{Pr}{1+R}\left(\sum_{i=0}^{M} c_i L_i^*(\eta)\right) \times \left(\sum_{i=1}^{M}\sum_{k=1}^{i} d_i\,\gamma_{i,k}^{(1)}\,\eta^{k-1}\right)^2 = 0. \quad (34)$$

We now collocate Eqs. (33) and (34) at $(M-n+1)$ points η_s, $s = 0, 1, \ldots, M-n$ as

$$\sum_{i=3}^{M}\sum_{k=3}^{i} c_i\,\gamma_{i,k}^{(3)}\,\eta_s^{k-3} + \sum_{i=0}^{M} c_i L_i^*(\eta_s)\left(\sum_{i=2}^{M}\sum_{k=2}^{i} c_i\,\gamma_{i,k}^{(2)}\,\eta_s^{k-2}\right) - \left(\frac{2m}{1+m}\right)\left(\sum_{i=1}^{M}\sum_{k=1}^{i} c_i\,\gamma_{i,k}^{(1)}\,\eta_s^{k-1}\right)^2 - D\sum_{i=1}^{M}\sum_{k=1}^{i} c_i\,\gamma_{i,k}^{(1)}\,\eta_s^{k-1} = 0, \quad (35)$$

$$\sum_{i=2}^{M}\sum_{k=2}^{i} d_i\,\gamma_{i,k}^{(2)}\,\eta_s^{k-2} + \epsilon\sum_{i=0}^{M} d_i L_i^*(\eta_s)\left(\sum_{i=2}^{M}\sum_{k=2}^{i} d_i\,\gamma_{i,k}^{(2)}\,\eta_s^{k-2}\right) + \epsilon\left(\sum_{i=1}^{M}\sum_{k=1}^{i} d_i\,\gamma_{i,k}^{(1)}\,\eta_s^{k-1}\right)^2 + \frac{Pr}{1+R}\left(\sum_{i=0}^{M} c_i L_i^*(\eta_s)\right) \times \left(\sum_{i=1}^{M}\sum_{k=1}^{i} d_i\,\gamma_{i,k}^{(1)}\,\eta_s^{k-1}\right)^2 = 0. \quad (36)$$

For suitable collocation points, we use roots of shifted Legendre polynomial $L_{M-n+1}^*(\eta)$. Also, by substituting formula (32) in the boundary conditions (19) and (20) we can obtain five equations as follows

Table 2. Comparison of the numerical value of $-f''(0)$, obtained by Legendre collocation method for $\alpha = 0.25, \lambda = 0$ with Fang et al. [15]

m	10.00	9.00	7.00	5.00	3.00	1.00	0.50	0.00	-1/3	-0.50
$-f''(0)$	1.1433	1.1404	1.1323	1.1186	1.0905	1.0000	0.9338	0.78439	0.5000	0.0833
Present work	1.1433	1.1404	1.1322	1.1186	1.0904	1.0000	0.9337	0.7843	0.5000	0.0832

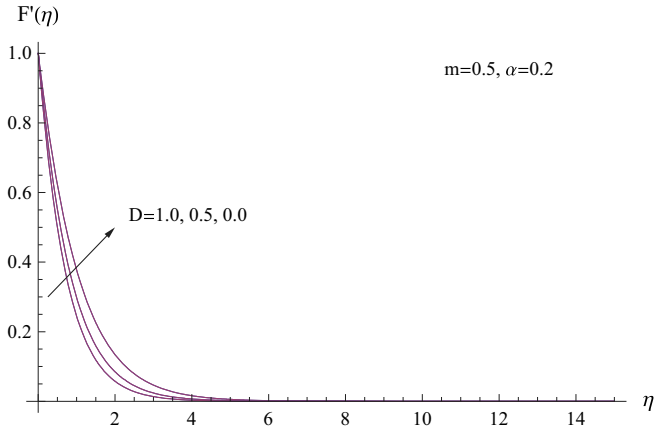

Figure 2. The behavior of the velocity distribution for various values of D

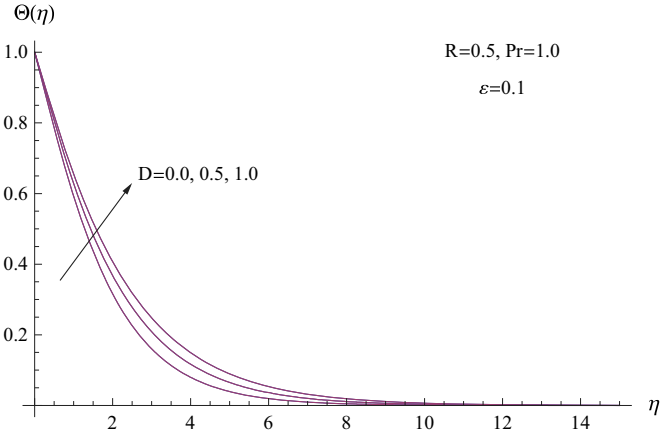

Figure 3. The behavior of the temperature distribution for various values of D

$$\sum_{i=0}^{M}(-1)^i c_i = \alpha\left(\frac{1-m}{1+m}\right), \quad \sum_{i=0}^{M}(-1)^i d_i = 1, \quad \sum_{i=0}^{M} d_i = 0, \quad \sum_{i=0}^{M} r_i c_i = 1, \quad \sum_{i=0}^{M} s_i c_i = 0, \tag{37}$$

where $r_i = L_i^{*'}(0),\ s_i = L_i^{*'}(\eta_\infty)$.

Eqs. (35) and (36), together with five equations of the boundary conditions (37), give a system of $(2M+2)$ algebraic equations which can be solved, for the unknowns $c_i,\ d_i,\ i = 0, 1, \ldots, M$, using Newton iteration method. In our numerical study we take $M = 5$, i.e., five terms of the truncated series solution (32), at $\eta_\infty = \hbar = 14$.

5. Results and Discussion

Tables 1 and 2 clearly reveal that present solution namely Legendre collocation method shows excellent agreement with the existing solutions in the literature [15]. This analysis shows that the proposed method suits for the

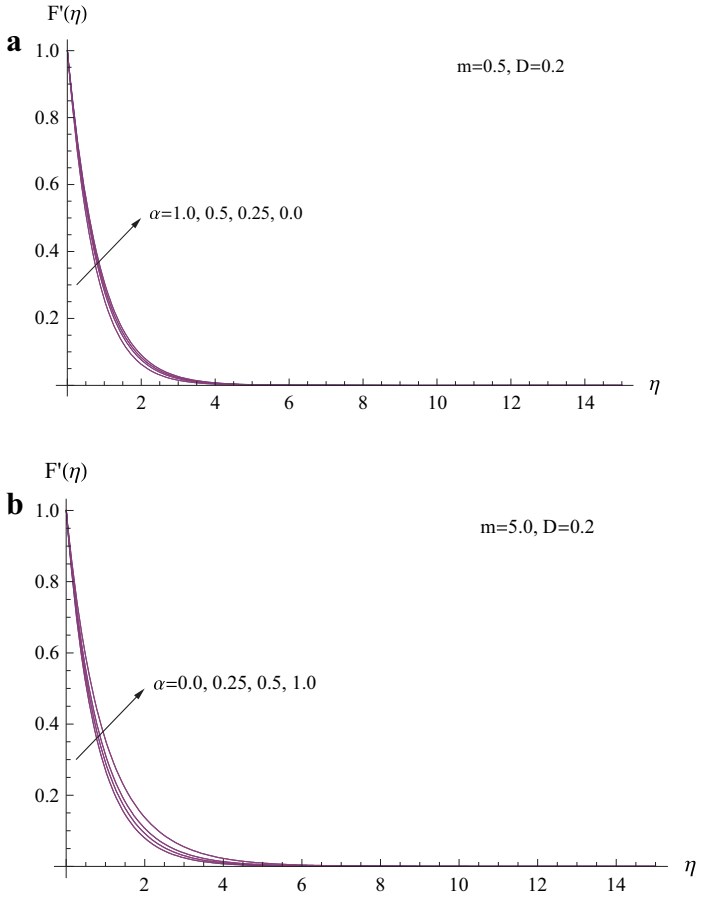

Figure 4. **a** The behavior of the velocity distribution for various values of α with $m = 0.5$. **b** The behavior of the velocity distribution for various values of α with $m = 5$

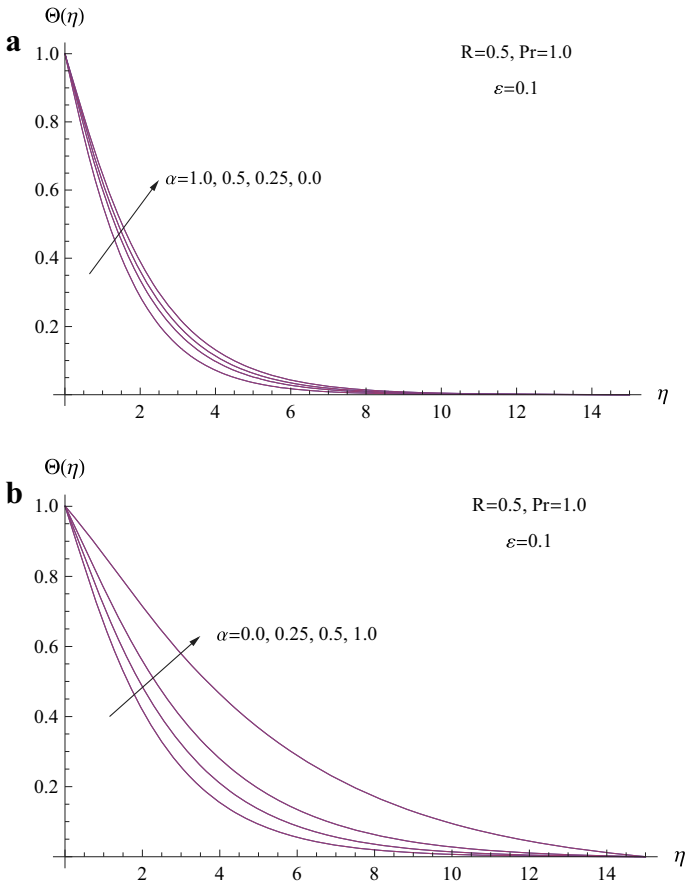

Figure 5. **a** The behavior of the temperature distribution for various values of α with $m = 0.5$. **b** The behavior of the temperature distribution for various values of α with $m = 5$

problems of boundary layer flow in fluid-saturated porous medium. This section provides the behavior of parameters involved in the expressions of heat transfer characteristics for the stretching sheet. Numerical evaluation for the solutions of this problem is performed and the results are illustrated graphically in Figs. 2, 3, 4, 5, 6, 7, 8, 9 and 10. The study of flow in porous media is very important in approximating the shape of spherical particles or cylindrical fibers which better fit the model of permeability assumed for the analysis. Effects of the porous parameter D on velocity and temperature profiles are shown in Figs. 2 and 3, respectively. It is observed that the velocity decreases for increasing values of porous parameter. Furthermore, the momentum boundary layer thickness decreases as porous parameter D increases. Figure 3 elucidates that the fluid temperature enhance with an increase in the porous parameter.

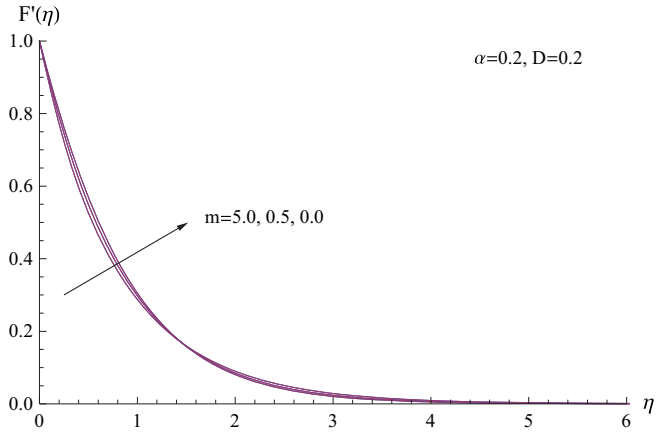

Figure 6. The behavior of the velocity distribution for various values of m

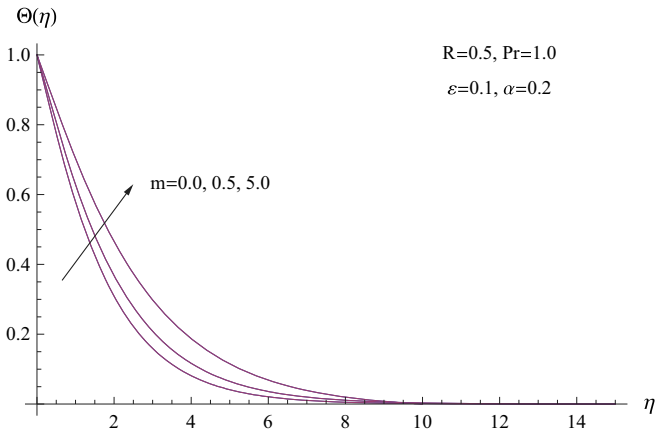

Figure 7. The behavior of the temperature distribution for various values of m

The effects of wall thickness parameter on the fluid flow and the temperature distribution have been analyzed and the results are presented in Figs. 4 and 5. From Fig. 4 it is clear that the velocity at any point near to the plate decreases as the wall thickness parameter increases for $m < 1$ and the reverse is true for $m > 1$. Also, it is obvious from these figures that the thickness of the boundary layer becomes thinner for a higher value of α when $m < 1$ and becomes thicker for a higher value of α when $m > 1$.

Figure 5 display that the wall thickness parameter decreased the thickness of the thermal boundary layer and enhanced the rate of heat transfer for $m < 1$ whereas reverse trend is observed as $m > 1$. Physically, increasing the value of α when $m < 1$ will decrease the flow velocity because under the variable wall thickness, not all the pulling force of the stretching sheet can

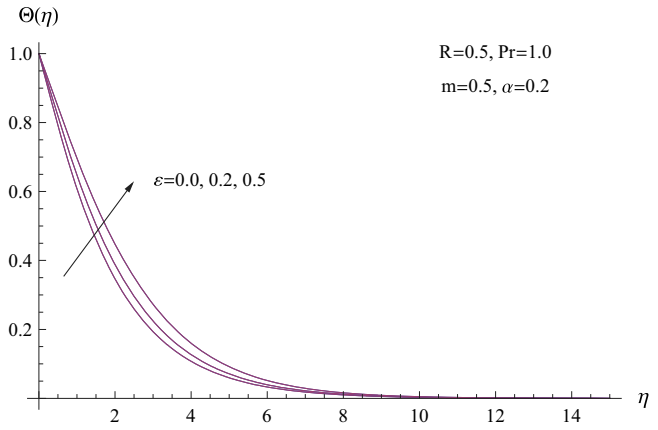

Figure 8. The behavior of the temperature distribution for various values of ϵ

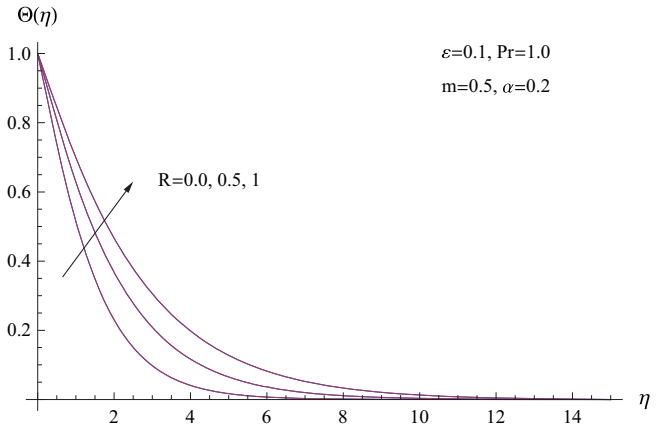

Figure 9. The behavior of the temperature distribution for various values of R

be transmitted to the fluid causing a decrease for both friction between the fluid layers and temperature distribution for the fluid. But, when $m > 1$ the velocity of the flow layers will increase causing an enhance for the friction force between this layers and thus increasing its temperature. Likewise, for a higher value of α, the thermal boundary layer becomes thinner when $m < 1$ compared with the case of $m > 1$.

Figure 6 shows that the velocity rises with a decrease in the values of the velocity power index m. This implies the momentum boundary thickness becomes thinner as the m increases along the sheet and the reverse is true away from it.

Figure 7 displays the influence of the velocity power index parameter m on the temperature profiles. It is clearly seen from this figure that increasing the value of m produces an increase in the temperature profiles. It further

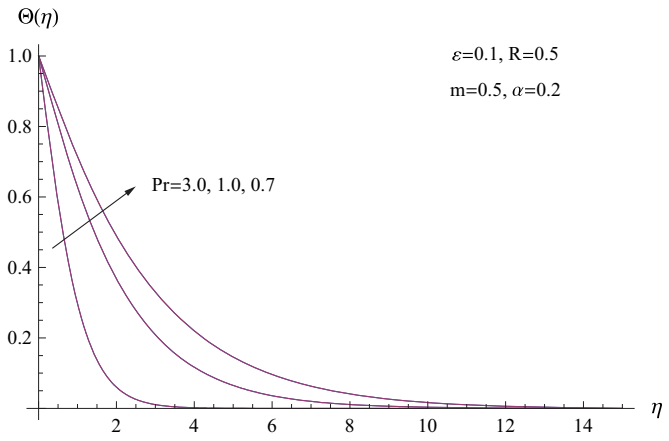

Figure 10. The behavior of the temperature distribution for various values of Pr

shows that the larger the value of m, the higher the magnitude of the thermal boundary thickness will be.

In Fig. 8 we have varied the thermal conductivity parameter ϵ keeping the values of all other parameters fixed. Figure 8 reveals that the temperature profile as well as the thickness of the thermal boundary layer increase when ϵ increases.

Figure 9 illustrates the effects of radiation parameter R on the temperature profiles when other parameters held constant. It is depicted that the temperature field and the thermal boundary layer thickness increase with the increase in R.

It is observed from Fig. 10 that an increase in the Prandtl number results in decreases the heat transfer profiles. The reason is that increasing values of Prandtl number equivalent to decreasing the thermal conductivities and therefore heat is able to diffuse away from the heated sheet more rapidly. Hence in the case of increasing Prandtl number, the boundary layer is thinner and the heat transfer is reduced.

Table 3 shows the influence of the porous parameter D, wall thickness parameter α, the velocity power index parameter m, the radiation parameter R, the Prandtl number Pr and thermal conductivity parameters ϵ on the local skin friction coefficient and the local Nusselt number. It is noticed that increases in the wall thickness parameter leads to an increase in both the local skin-friction coefficient and the local Nusselt number. Likewise, the local Nusselt number is reduced but the skin-friction coefficient is increased with increasing for both values of porous parameter and velocity power index parameter. Also, an increase in the Prandtl number causes an increase in the local Nusselt number. This is because a fluid with larger Prandtl number possesses larger heat capacity, and hence intensifies the heat transfer. Moreover, it is observed that the values of the local Nusselt number decreases with increase in both the thermal conductivity parameter and the radiation parameter.

Table 3. Values of $-f''(0)$ and $-\theta'(0)$ for various values of $D, \alpha, m, \epsilon, R$ and Pr

D	α	m	ϵ	R	Pr	$-f''(0)$	$-\theta'(0)$
0.0	0.2	0.5	0.1	0.5	1.0	0.92482	0.441838
0.5	0.2	0.5	0.1	0.5	1.0	1.16858	0.401882
1.0	0.2	0.5	0.1	0.5	1.0	1.36982	0.372258
0.5	0.0	0.5	0.1	0.5	1.0	1.13387	0.375148
0.5	0.25	0.5	0.1	0.5	1.0	1.17740	0.408670
0.5	0.5	0.5	0.1	0.5	1.0	1.22242	0.443211
0.5	1.0	0.5	0.1	0.5	1.0	1.31682	0.515101
0.5	0.2	0.0	0.1	0.5	1.0	1.04487	0.472745
0.5	0.2	0.5	0.1	0.5	1.0	1.16858	0.401882
0.5	0.2	5.0	0.1	0.5	1.0	1.32780	0.303396
0.5	0.2	0.5	0.0	0.5	1.0	1.16858	0.434823
0.5	0.2	0.5	0.2	0.5	1.0	1.16858	0.373956
0.5	0.2	0.5	0.5	0.5	1.0	1.16858	0.310624
0.5	0.2	0.5	0.1	0.0	1.0	1.16858	0.547732
0.5	0.2	0.5	0.1	0.5	1.0	1.16858	0.401882
0.5	0.2	0.5	0.1	1.0	1.0	1.16858	0.319550
0.5	0.2	0.5	0.1	0.5	0.7	1.16858	0.302207
0.5	0.2	0.5	0.1	0.5	1.0	1.16858	0.401882
0.5	0.2	0.5	0.1	0.5	3.0	1.16858	0.896313

6. Conclusions

In this paper, the Legendre collocation method is used to investigate the approximate solution of the resulting non-linear system of ODEs for the problem of flow and heat transfer in a quiescent Newtonian fluid flow caused solely by a stretching sheet which embedded in a porous medium with variable thickness, variable thermal conductivity and thermal radiation. The fluid thermal conductivity is assumed to vary as a linear function of temperature. Comparison with previously published work was performed and the results were found to be in excellent agreement. Asystematic study on the effects of the various parameters on flow and heat transfer characteristics is carried out. It was found that the effect of increasing values of the porous parameter, the velocity power index parameter, thermal conductivity parameter and the radiation parameter reduce the local Nusselt number. On the other hand it was observed that the local Nusselt number increases as the Prandtl number and wall thickness parameter increases. Moreover, it is interesting to find that as the porous parameter, wall thickness parameter and the velocity power index parameter increases in magnitude, causes the fluid to slow down past the stretching sheet, the skin-friction coefficient increases in magnitude. From the presented results, we can see that the numerical solution is in excellent agreement with those obtained by other methods.

References

[1] Crane, L.J.: Flow past a stretching plate. Z. Angew. Math. Phys. **21**, 645–647 (1970)

[2] Gupta, P.S., Gupta, A.S.: Heat and mass transfer on a stretching sheet with suction or blowing. Can. J. Chem. Eng. **55**(6), 744–746 (1979)

[3] Soundalgekar, V.M., Ramana, T.V.: Heat transfer past a continuous moving plate with variable temperature. Warme-Und Stoffuber Tragung. **14**, 91–93 (1980)

[4] Grubka, L.J., Bobba, K.M.: Heat transfer characteristics of a continuous stretching surface with variable temperature. J. Heat Transf. **107**, 248–250 (1985)

[5] Chen, C.K., Char, M.: Heat transfer on a continuous stretching surface with suction or blowing. J. Math. Anal. Appl. **35**, 568–580 (1988)

[6] Hayat, T., Abbas, Z., Javed, T.: Mixed convection flow of a micropolar fluid over a non-linearly stretching sheet. Phys. Lett. A **372**, 637–647 (2008)

[7] Cheng, P., Minkowycz, W.J.: Free convection about a vertical flat plate embedded in a porous medium with application to heat transfer from a dike. J. Geophys. Res. **82**, 2040–2044 (1977)

[8] Elbashbeshy, E.M.A., Bazid, M.A.A.: Heat transfer in a porous medium over a stretching surface with internal heat generation and suction or injection. Appl. Math. Comp. **158**, 799–807 (2004)

[9] Cortell, R.: Flow and heat transfer of a fluid through a porous medium over a stretching surface with internal heat generation/absorption and suction/blowing. Fluid Dyn. Res. **37**, 231–245 (2005)

[10] Hayat, T., Abbas, Z., Pop, I., Asghar, S.: Effects of radiation and magnetic field on the mixed convection stagnation-point flow over a vertical stretching sheet in a porous medium. Int. J. Heat Mass Transf. **53**, 466–474 (2010)

[11] Hossain, M.A., Alim, M.A., Rees, D.: The effect of radiation on free convection from a porous vertical plate. Int. J. Heat Mass Transf. **42**, 181–191 (1999)

[12] Elbashbeshy, E.M.A., Dimian, M.F.: Effects of radiation on the flow and heat transfer over a wedge with variable viscosity. Appl. Math. Comput. **132**, 445–454 (2002)

[13] Abel, M.S., Mahesha, N.: Heat transfer in MHD viscoelastic fluid flow over a stretching sheet with variable thermal conductivity, non-uniform heat source and radiation. Appl. Math. Model. **32**, 1965–1983 (2008)

[14] Bataller, R.C.: Radiation effects in the Blasius flow. Appl. Math. Comput. **198**, 333–338 (2008)

[15] Fang, T., Zhang, J., Zhong, Y.: Boundary layer flow over a stretching sheet with variable thickness. Appl. Math. Comput. **218**, 7241–7252 (2012)

[16] Al-Housseiny, T.T., Stone, H.A.: On boundary-layer flows induced by the motion of stretching surfaces. J. Fluid Mech. **706**, 597–606 (2012)

[17] Fang, T., Tarek, M.A.E.L.: Self-similar flow due to the stretching of a deformable fiber. Eur. Phys. J. Plus **129**, 252 (2014)

[18] Khader, M.M.: On the numerical solutions for the fractional diffusion equation. Commun. Nonlinear Sci. Numer. Simul. **16**, 2535–2542 (2011)

[19] Khader, M.M., Hendy, A.S.: The approximate and exact solutions of the fractional-order delay differential equations using Legendre pseudo-spectral method. Int. J. Pure Appl. Math. **74**(3), 287–297 (2012)

[20] Khader, M.M., Sweilam, N.H., Mahdy, A.M.S.: Numerical study for the fractional differential equations generated by optimization problem using Chebyshev collocation method and FDM. Appl. Math. Inf. Sci. **7**(5), 2013–2020 (2013)

[21] Bell, W.W.: Special Functions for Scientists and Engineers. Great Britain, Butler and Tanner Ltd, Frome and London (1968)

[22] Sweilam, N.H., Khader, M.M.: A Chebyshev pseudo-spectral method for solving fractional order integro-differential equations. ANZIAM **51**, 464–475 (2010)

[23] Sweilam, N.H., Khader, M.M., Mahdy, A.M.S.: Numerical studies for fractional-order Logistic differential equation with two different delays. J. Appl. Math. **2012**, 1–14 (2012)

[24] Khader, M.M., Hendy, A.S.: A new Legendre computational matrix method: An application for solving the high order fractional differential equations. Walailak J. Sci. Technol. **11**(4), 289–305 (2014)

[25] Raptis, A.: Flow of a micropolar fluid past a continuously moving plate by the presence of radiation. Int. J. Heat Mass Transf. **41**, 2865–2866 (1998)

[26] Raptis, A.: Radiation and viscoelastic flow. Int. Commun. Heat Mass Transf. **26**, 889–895 (1999)

[27] Chiam, T.C.: Magnetohydrodynamic heat transfer over a non-isothermal stretching sheet. Acta Mech. **122**, 169–179 (1997)

[28] Mahmoud, M.A.A., Megahed, A.M.: MHD flow and heat transfer in a non-Newtonian liquid film over an unsteady stretching sheet with variable fluid properties. Can. J. Phys. **87**, 1065–1071 (2009)

[29] Das, K.: A mathematical model on magnetohydrodynamic slip flow and heat transfer over a non-linear stretching sheet. Therm. Sci. **18**(2), S475–S488 (2014)

M. M. Khader
Department of Mathematics and Statistics
College of Science
Al-Imam Mohammad Ibn Saud Islamic University (IMSIU)
Riyadh
Saudi Arabia

and

Department of Mathematics
Faculty of Science
Benha University
Benha
Egypt
e-mail: mohamedmbd@yahoo.com;
mohamed.khader@fsc.bu.edu.eg

Received: November 8, 2014.

Revised: May 4, 2015.

Accepted: June 4, 2015.